# A spectral element method for wave propagation simulation near a fluid-solid interface

Dimitri Komatitsch[1], Christophe Barnes[2], Jeroen Tromp[1],

(1) Harvard University, Cambridge, USA (e-mail: komatits@seismology.harvard.edu). (2) Institut de Physique du Globe de Paris, France (e-mail: barnes@ipgp.jussieu.fr).

## Abstract

**We introduce a spectral element method for modeling wave propagation in media with both fluid (acoustic) and solid (elastic) regions, as in offshore seismic experiments. The problem is formulated in terms of displacement in elastic regions and a velocity potential in acoustic regions. Matching between domains is implemented based upon an interface integral in the framework of a predictor-multicorrector iterative time scheme.**

## Formulation of the problem

We consider a linear elastic rheology for the heterogeneous solid, while the fluid is assumed to be inviscid and of constant density.

$$
\begin{aligned}
\rho\ddot{\mathbf{u}} &= \boldsymbol{\nabla}\cdot\boldsymbol{\sigma} + \mathbf{f} \ , \\
\boldsymbol{\sigma} &= \mathbf{C}:\boldsymbol{\varepsilon} = \lambda\mathrm{tr}(\boldsymbol{\varepsilon})\mathbf{I} + 2\mu\boldsymbol{\varepsilon} \ , \\
\boldsymbol{\varepsilon} &= \tfrac{1}{2}[\boldsymbol{\nabla}\mathbf{u} + (\boldsymbol{\nabla}\mathbf{u})^T] \ ,
\end{aligned}
\tag{1}
$$

The wavefield in the acoustic, inviscid fluid is governed by the conservation and dynamics equations (e.g., [7])

$$
\begin{aligned}
\rho\dot{\mathbf{v}} + \boldsymbol{\nabla} p &= \mathbf{0} \ , \\
\dot{p} + \rho c^2 \boldsymbol{\nabla}\cdot\mathbf{v} &= 0 \ ,
\end{aligned}
\tag{2}
$$

where $\mathbf{v}$ denotes the velocity vector, $p$ pressure, and $c$ the speed of acoustic waves. Assuming that the density $\rho$ is constant, we have $\boldsymbol{\nabla}\times\mathbf{v} = \mathbf{0}$. Thus the velocity $\mathbf{v}$ can be written as the gradient of a scalar potential $\phi$ [7]. Substituting the definition $\mathbf{v} = \boldsymbol{\nabla}\phi$ in (2), we can eliminate pressure and obtain a second-order system

$$
\nabla^2\phi = c^{-2}\ddot{\phi} \ .
\tag{3}
$$

To couple the two media at a fluid-solid interface, we have to ensure the continuity of traction $\boldsymbol{\tau} = \boldsymbol{\sigma}\cdot\hat{\mathbf{n}}$. From (2) we see that the pressure $p$ equals $-\rho\dot{\phi}$, which implies that the continuity of traction may be expressed as

$$
\boldsymbol{\tau} = \rho\dot{\phi}\,\hat{\mathbf{n}} \ .
\tag{4}
$$

The kinematic boundary condition of continuity of the normal component of velocity is

$$
\hat{\mathbf{n}}\cdot\boldsymbol{\nabla}\phi = \hat{\mathbf{n}}\cdot\dot{\mathbf{u}} \ .
\tag{5}
$$

## Discretization

We rewrite the above coupled system of equations in a variational or weak form, by multiplying with test functions and integrating by part

$$\int_{\Omega_s} \rho \mathbf{w} \cdot \ddot{\mathbf{u}} \, d\Omega \;+\; \int_{\Omega_s} \boldsymbol{\nabla}\mathbf{w} : \mathbf{C} : \boldsymbol{\nabla}\mathbf{u} \, d\Omega$$
$$-\; \int_{\Gamma_i} \rho \mathbf{w} \cdot \hat{\mathbf{n}} \, \dot{\phi} \, d\Gamma - \int_{\Gamma_{abs}^s} \mathbf{w} \cdot \boldsymbol{\tau} \, d\Gamma = \mathbf{0} \;, \tag{6}$$

$$\int_{\Omega_f} c^{-2} w \ddot{\phi} \, d\Omega \;+\; \int_{\Omega_f} \boldsymbol{\nabla} w \cdot \boldsymbol{\nabla}\phi \, d\Omega$$
$$+\; \int_{\Gamma_i} w \, \dot{\mathbf{u}} \cdot \hat{\mathbf{n}} \, d\Gamma + \int_{\Gamma_{abs}^f} c^{-1} w \dot{\phi} \, d\Gamma = \int_{\Omega_f} w f \, d\Omega \;. \tag{7}$$

The solid and fluid regions of the model are denoted by $\Omega_s$ and $\Omega_f$ respectively, $\Gamma_{abs}^f$ denotes the acoustic absorbing boundary, $\Gamma_{abs}^s$ denotes the elastic absorbing boundary, and $\Gamma_i$ denotes the interface between the two media. This weak formulation of the problem forms the basis for the spatial and temporal discretization of the problem in the next two sections using the spectral element method (SEM). For more details regarding SEM, the reader can refer to [8, 6, 4, 5].

## Spatial discretization

We introduce a Legendre spectral element discretization of the variational problem (6)–(7). The domain $\Omega$ is first meshed in terms of a set of $n_{el}$ non-overlapping elements $\Omega_e$, as in a classical FEM. Each of these elements is individually mapped to a reference domain $\Lambda = [-1,1]^{n_d}$ based upon an invertible local mapping $\mathcal{F}_e$. On the reference element $\Lambda$ we introduce a set of local basis functions that provide accuracy of order $N$ for the solution. We choose this set of functions to be polynomials of degree $N$. We introduce a set of $N+1$ points $\xi_i, \in [-1,1]$, called the Gauss-Lobatto-Legendre (GLL) points. We subsequently choose the set of basis functions to be the $N+1$ Lagrange interpolants $h_p(\xi)$. All the integrals appearing in (6)–(7) may be approximated at the element level using GLL quadrature:

$$\int_{\Omega} uw \, d\Omega \;=\; \sum_{e=1}^{n_{el}} \int_{\Omega_e} uw \, d\Omega$$
$$\simeq\; \sum_{e=1}^{n_{el}} \sum_{i=0}^{N} \sum_{j=0}^{N} \omega_i \omega_j J_e(\xi_i, \eta_j) u^e(\xi_i, \eta_j) w^e(\xi_i, \eta_j) \;, \tag{8}$$

where $\omega_i > 0$ are the weights of the classical GLL quadrature that can be computed numerically [2], and $J_e$ is the Jacobian associated with the mapping $\mathcal{F}_e$. Let $\mathbf{w}_N = (w_x, w_z)^T$, $w_N$, $\mathbf{u}_N = (u_x, u_z)^T$ and $\phi_N$ denote the piecewise-polynomial approximations of the test-functions. The discrete variational problem to be solved can thus be expressed as: for all time $t$, find $\mathbf{u}_N$ and $\phi_N$ such that for all $\mathbf{w}_N$ and $w_N$ we have

$$(\mathbf{w_N}, \ddot{\mathbf{u}}_N) + a_s(\mathbf{w}_N, \mathbf{u}_N) - A_s(\mathbf{w}_N, \phi_N)_{\Gamma_i} \;=\; (\mathbf{w}_N, \boldsymbol{\tau}_N)_{\Gamma_{abs}^s} \;,$$
$$(w_N, \ddot{\phi}_N) + a_f(w_N, \phi_N) + A_f(w_N, \mathbf{u}_N)_{\Gamma_i} \;=\; (w_N, \phi_N)_{\Gamma_{abs}^f} + (w_N, f_N) \;. \tag{9}$$

Time discretization of the resulting system of second-order ordinary differential equations is achieved using a classical implicit Newmark scheme written in a predictor/multicorrector format [3]. For a general second-order system of the form

$$M\ddot{\mathbf{d}} + C\dot{\mathbf{d}} + K\mathbf{d} = F \;, \tag{10}$$

the scheme is written as

$$M\ddot{\mathbf{d}}_{n+1} + C\dot{\mathbf{d}}_{n+1} + K\mathbf{d}_{n+1} = F_{n+1} \ , \tag{11}$$

where

$$\mathbf{d}_{n+1} = \mathbf{d}_n + \Delta t \dot{\mathbf{d}}_n + \frac{\Delta t^2}{2}[(1 - 2\beta)\ddot{\mathbf{d}}_n + 2\beta\ddot{\mathbf{d}}_{n+1}] \ , \tag{12}$$

and

$$\dot{\mathbf{d}}_{n+1} = \dot{\mathbf{d}}_n + \Delta t[(1 - \gamma)\ddot{\mathbf{d}}_n + \gamma\ddot{\mathbf{d}}_{n+1}] \ . \tag{13}$$

The scheme is applied to advance in time both the displacement in the solid and the velocity potential in the fluid. At the initial time $t = 0$, zero initial conditions are assumed i.e., $\mathbf{d} = \mathbf{0}$ and $\dot{\mathbf{d}} = \mathbf{0}$.

## Numerical tests for a flat interface

We consider two homogeneous half-spaces in contact at a flat interface. The lower part of the model is elastic, with $c_p = 3400$ m/s, $c_s = 1963$ m/s and $\rho = 2500$ kg/m$^3$, while the upper part is acoustic, a water layer. The size of each domain is $6.4 \times 2.4$ km. We use a total of $120 \times 90 = 10800$ spectral elements. The polynomial degree is $N = 5$, therefore the total number of points of the global mesh is 271051. Absorbing conditions are used on all the edges of the grid to simulate two half-spaces. The source time function is a Ricker wavelet with dominant frequency $f_0 = 10$ Hz. The minimum number of points per wavelength is close to 5. In practice, the implicit Newmark scheme converges after 3 corrector iterations at each time step. The source is placed at a distance of $z_s = 500$ m above the interface. The 110 receivers are located on a horizontal line at a distance of $z_r = 533.33$ m above the interface and at a horizontal offset from the source varying between 925 m and 4425 m.
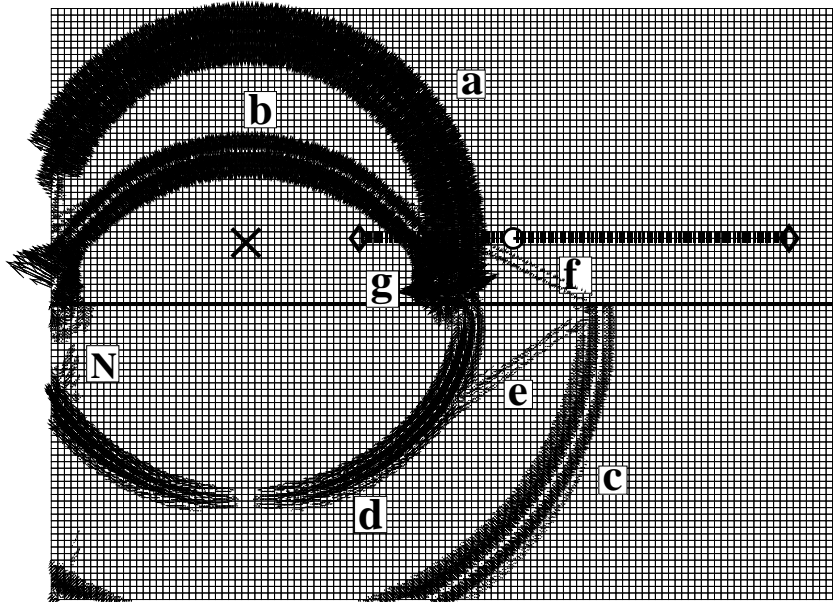


Figure 1: Snapshot of the velocity vector at time $t = 1.26$ s. The cells shown represent the mesh of spectral elements. The size of the domain is $6.4 \times 4.8$ km. The direct (a) and reflected (b) $P$ waves can be observed in the fluid, the transmitted $P$ (c) and $P$-to-$S$ converted (d) waves are clearly visible in the solid. Significant refracted waves are also present (e,f,g) as well as spurious reflections on the absorbing boundaries (N).

Figure 1 shows the acquisition geometry and a snapshot of the velocity vector field at time $t = 1.26$ s. Several phases can be distinguished:

(a) the direct $P$ wave,

(b) the reflected $P$ wave,

(c) the transmitted $P$ wave,

(d) the $P$-to-$S$ converted wave,

(e) the $P$ refracted wave converted to $S$-wave in the solid,

(f) the $P$ refracted wave in the fluid,

(g) the $S$ refracted wave converted to $P$-wave in the fluid.

We now compare the numerical solution obtained with our SEM to the analytical solution of the problem. The comparison is performed at receiver #40. The horizontal and vertical components of the numerical and analytical velocity are shown almost superimposed in Figure 2. The difference between the two curves is also shown in the same plot using an amplification factor of 5. The agreement is very good for all phases, which further validates the method.
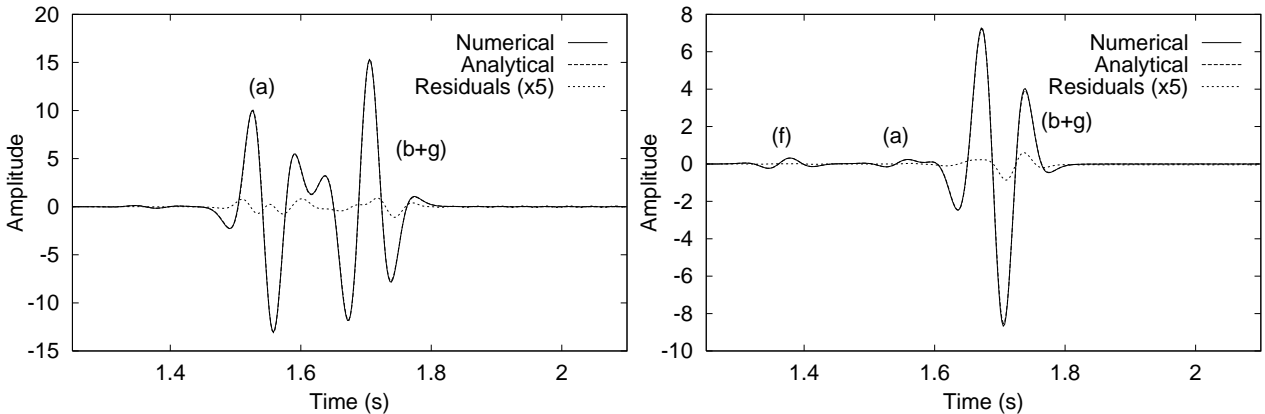


Figure 2: Horizontal (left) and vertical (right) components of velocity recorded at receiver #40. The solid line represents the numerical solution, the dashed line, which is almost perfectly superimposed to the solid line, is the analytical solution, and the dotted line is the difference between the two curves amplified by a factor of 5. The agreement is excellent.

## Numerical test for a sinusoidal interface

We now consider a model of the sea floor with strong sinusoidal topography. A free surface is implemented at the surface of the sea, an absorbing condition at the bottom of the solid, and periodic conditions on the vertical sides of the region of interest. All model parameters remain the same as before. The source is located at $x_s = 2908.33$ m at a depth of $z_s = 1700$ m below the surface of the sea. The line of receivers is composed of 50 receivers going from $x_{r_1} = 3200$ m to $x_{r_{50}} = 5400$ m at a depth of $z_r = 1500$ m. The horizontal mesh follows the shape of the sea floor in order to be able to impose the matching condition between domains at the sinusoidal interface. The length of the records is 2.1 s and the time step is $\Delta t = 0.7$ ms; therefore the total number of time steps is 3000.

The snapshot of the velocity vector shown in Figure 3 illustrates the complexity of the wave field, in particular the presence of curved reflected and transmitted waves, triplications, and interface waves. The main phases that can be distinguished are:
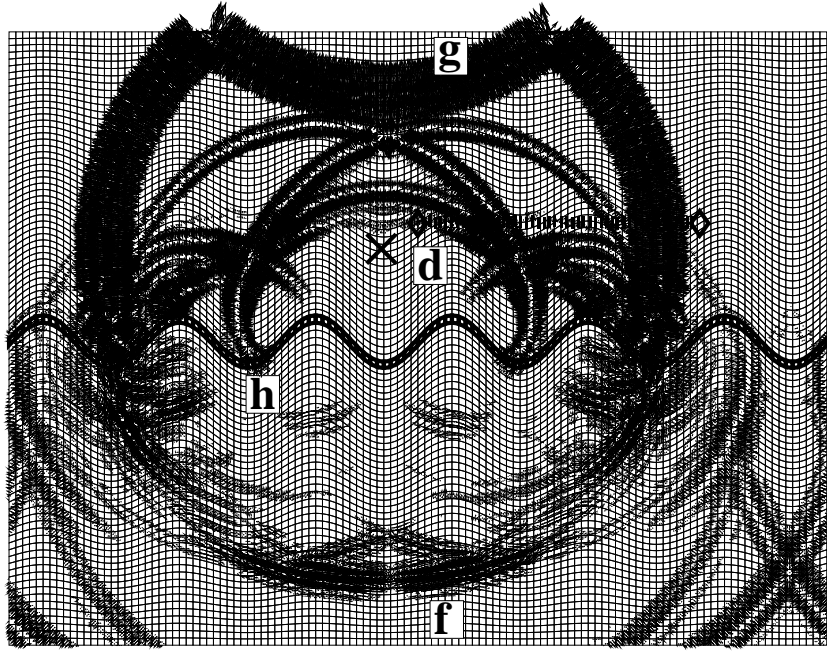
Figure 3: Snapshot of the velocity vector for a sea bottom with strong sinusoidal topography. Strongly curved reflected waves, triplications due to the topography of the sea floor (d), transmitted *P*-waves and transmitted *S*-waves (f) can be observed. The direct *P*-wave undergoes total reflection at the surface of the sea (g). The slow event traveling along the sea floor on the second snaphot (h) is interpreted as a Stoneley wave.

(a) the direct *P*-wave,

(b) the strongly curved reflected *P*-wave on the first anticline on the right,

(c) the *P*-wave reflected off the first anticline on the left (symmetric of phase (b)),

(d) the *P*-wave reflected off the central syncline, which undergoes a time delay and therefore a triplication,

(e) various transmitted *P*-waves,

(f) various transmitted *P*-to-*S* converted waves,

(g) the *P*-wave reflected at the surface of the sea,

(h) a slow phase traveling along the interface, which is interpreted to be Stoneley wave [1].

## Conclusions

We have shown that the use of a velocity potential in homogeneous acoustic regions allows to use the spectral element method for modeling wave propagation near a fluid-solid interface. Correct matching conditions between the fluid and the solid regions are enforced based upon a weak formulation of the interface equations. The discrete system obtained is solved in the context of an implicit iterative time scheme. Good accuracy is obtained for a test case with flat interface. The method is robust when strong interface topography is present.

## Acknowledgments

# References

[1] M. A. Biot. The interaction of Rayleigh and Stoneley waves in the ocean bottom. *Bull. Seis. Soc. Am.*, 42:81–93, 1952.

[2] C. Canuto, M. Y. Hussaini, A. Quarteroni, and T. A. Zang. *Spectral methods in fluid dynamics*. Springer-Verlag, New York, 1988.

[3] Thomas J. R. Hughes. *The finite element method, linear static and dynamic finite element analysis*. Prentice-Hall International, Englewood Cliffs, NJ, 1987.

[4] D. Komatitsch and J. P. Vilotte. The Spectral Element method: an efficient tool to simulate the seismic response of 2D and 3D geological structures. *Bull. Seis. Soc. Am.*, 88(2):368–392, 1998.

[5] D. Komatitsch, J. P. Vilotte, R. Vai, J. M. Castillo-Covarrubias, and F. J. Sánchez-Sesma. The Spectral Element method for elastic wave equations: application to 2D and 3D seismic problems. *Int. J. Num. Meth. Eng.*, 1999. in press.

[6] Dimitri Komatitsch. *Méthodes spectrales et éléments spectraux pour l'équation de l'élastodynamique 2D et 3D en milieu hétérogène*. PhD thesis, Institut de Physique du Globe de Paris, Paris, France, 1997. May 1997.

[7] L. D. Landau and E. M. Lifshitz. *Fluid mechanics*. Pergamon Press, New-York, 1959.

[8] E. Priolo, J. M. Carcione, and G. Seriani. Numerical simulation of interface waves by high-order spectral modeling techniques. *J. Acoust. Soc. Am.*, 95(2):681–693, 1994.